Journal of Biomedical Optics

SPIEDigitalLibrary.org/jbo

Twenty-four-hour ambulatory recording of cerebral hemodynamics, systemic hemodynamics, electrocardiography, and actigraphy during people's daily activities

Quan Zhang
Vladimir Ivkovic
Gang Hu
Gary E. Strangman

SPIE

Twenty-four-hour ambulatory recording of cerebral hemodynamics, systemic hemodynamics, electrocardiography, and actigraphy during people's daily activities

Quan Zhang,[a,b,*] Vladimir Ivkovic,[a] Gang Hu,[a] and Gary E. Strangman[a,b]
[a]Massachusetts General Hospital, Harvard Medical School Neural Systems Group, 13th Street, Building 149, Room 2651, Charlestown, Massachusetts 02129
[b]Center for Space Medicine, Baylor College of Medicine, Houston, Texas

Abstract. The feasibility and utility of wearable 24-h multimodality neuromonitoring during daily activities are demonstrated. We have developed a fourth-generation ambulatory near infrared spectroscopy device, namely NINscan 4. NINscan 4 enables recording of brain function (via cerebral hemodynamics), systemic hemodynamics, electrocardiography, and actigraphy simultaneously and continuously for up to 24 h at 250-Hz sampling rate, during (and with minor restriction to) daily activities. We present initial 24-h human subject test results, with example analysis including (1) comparison of cerebral perfusion and oxygenation changes during wakefulness and sleep over a 24-h period and (2) capturing of hemodynamic changes prior, during and after sudden waken up in the night during sleep. These results demonstrate the first ambulatory 24-h cerebral and systemic hemodynamics monitoring, and its unique advantages including long-term data collection and analysis capability, ability to catch unpredictable transient events during activities of daily living, as well as coregistered multimodality analysis capabilities. These results also demonstrate that NINscan 4's motion artifact at 1-*g* head movement is smaller than physiological hemodynamic fluctuations during motionless sleep. The broader potential of this technology is also discussed. [DOI: 10.1117/1.JBO.19.4.047003]

Keywords: wearable neuromonitoring; near-infrared spectroscopy; tissue oxygenation; brain function; circadian; sleep.

Paper 130916R received Dec. 30, 2013; revised manuscript received Mar. 1, 2014; accepted for publication Mar. 5, 2014; published online Apr. 28, 2014.

1 Introduction

Cerebral hemodynamics—including blood volume, perfusion, and oxygenation levels—represent important measurements of brain function in many clinical and research applications, ranging from brain injury,[1] epilepsy,[2] stroke,[3] sleep disorders,[4] and psychiatric disorders such as depression and anxiety,[5,6] to circadian physiology and psychology studies, and behavioral science.[7,8] Typically, cerebral hemodynamics must be measured in a well-controlled lab environment, often via functional magnetic resonance imaging (fMRI) or positron emission tomography scans. However, the traditional short-term laboratory measurement of brain hemodynamics has several disadvantages. First, lab measurements cannot meet the need for diagnosis based on long-term recordings (e.g., many hours or days), such as those in the diagnosis of sleep disorders, or the study of circadian cycle. Second, for pathological conditions with transient symptoms, short-term measurements provide a low probability for catching the symptom; examples include epileptic seizure, sleep apnea, syncope, and hot flashes. And third, in some applications, lab measurement actually introduces unwanted interruption or distortion of activity or the results, where typical examples include sleep monitoring and behavioral studies that require substantial motion. Often patients have difficulties falling asleep in unfamiliar environments such as a sleep lab, making the home diagnosis a more ecologically-relevant choice. For behavioral scientists, the capability to monitor subjects' brain function during daily activities could greatly expand their potential domains of inquiry.

Near-infrared spectroscopy (NIRS) and diffuse optical imaging (DOI) have been explored in the latest three decades,[9,10] and researchers have just celebrated the 20th year of functional NIRS.[11] Despite promises otherwise, in most settings NIRS and DOI are still performed using large bedside time domain, frequency domain, or continuous wave methods, with instruments weighing tens or even hundreds of pounds.[9] Gradually, more portable NIRS devices have been developed.[12–15,16] However, most of these portable devices were still designed for short term measurements; basically, they were miniaturized bedside devices, not capable of ambulatory long-term data collection. In recent years, more advanced battery-powered portable NIRS devices have been developed,[17–24] and human subject data from monitoring during real life activities outside the lab environment have been investigated, such as during parabolic flight and high altitude hiking[24] and outdoor bicycle riding.[19] Most recently, a few NIRS device manufactures have made portable or even wearable NIRS devices commercially available, including HEO 200, PortaLite, NIRSport, and others (see reviews in Refs. 9–11 and 25). However, so far no continuous 24-h human subject monitoring data during real life activities has been reported.

The research-based NINscan 2 device was specifically designed as a wearable NIRS technology.[24] Now, a fourth generation device, NINscan 4, has been developed and is

*Address all correspondence to: Quan Zhang, E-mail: qzhang@nmr.mgh.harvard.edu

0091-3286/2014/$25.00

beginning to be used in a range of research studies. Comparing with other existing portable NIRS systems, NINscan 4 has lower electrical and motion-related noise, long-recording time (more than 24 h), friendly user interface (including event buttons for logging of events during ambulatory recording), and multimodality monitoring capability. Given the unique power of long term and wearable NIRS recordings, the term ambulatory NIRS (aNIRS) was coined;[24] however, the unique capabilities of aNIRS—particularly the long-term monitoring during daily activities—still need in depth and experimental demonstration.

2 Significance of Multimodality Monitoring

Studying a physiological phenomenon or diagnosis of a pathological condition often requires more than one type of measurement. Importantly, long-term ambulatory cerebral and systemic hemodynamic monitoring is new; in order to better explain and understand such measurements, it can be helpful to relate those measurements to other well understood parameters and established monitoring modalities. In NINscan 4, we implemented simultaneous actigraphy and electrocardiography (ECG) monitoring.

Actigraphy has been used to study sleep/wake and circadian patterns for 30 years,[26] has been used to distinguish wakefulness and sleep,[27,28] and it has also been used clinically as an adjunct assessment of sleep disorders and/or certain psychiatric conditions.[29–31] In sports medicine actigraphy is used to measure steps taken, distance walked, calories burned, floors climbed, and activity duration and intensity.[32]

ECG is a second parameter that can provide useful information related to cerebral hemodynamics. Cardiac and respiratory activities are the two most visible components in cerebral and systemic hemodynamics. Heart rate, derived from ECG, is a sensitive indicator of people's activity intensity; one can also derive respiration signal from ECG.[33,34] Long-term ambulatory ECG monitoring, also called Holter monitoring or ambulatory ECG, is a major subfield in cardiology and is a routine procedure for detection and diagnosis of many disorders characterized by intermittent or rare cardiac symptoms (e.g., arrhythmias, transient ischemic episodes, and silent myocardial ischemia).[35,36] Heart rate variability analysis further provides information about sympathetic and the parasympathetic nervous system,[37] which can be further correlated with cerebral and systemic hemodynamics. It has even been suggested that a sleep spectrogram derived from ECG can be used to dynamically track cardiopulmonary interactions, and provide a complementary approach to the conventional characterization of graded nonrapid eye movement sleep stages.[38] Therefore, simultaneous ECG monitoring can provide rich physiological and/or pathological information, which can potentially be used to help the hemodynamic analysis.

To demonstrate both the feasibility and utility of wearable 24-h monitoring, we performed preliminary tests on healthy human subjects while simultaneously recording aNIRS, ECG and accelerometry/actigraphy.

3 Methods

3.1 *NINscan 4 Multimodality Monitoring and Recording*

In our NINscan system designs, we have attempted to maximize the range of monitoring environment and minimize the perturbation to subject's normal activities. Considering the broad potential applications, we extended NINscan's monitoring and recording time to increase the opportunities to catch unpredictable transient events, and implemented several auxiliary physiological monitoring channels so that for a specific application, NINscan data collection can be as fully self-contained, complete, and independent as possible. Besides the small form factor and motion resistance, our NINscan series includes two key features. First, among these is long term and independent data collection capabilities. With its internal memory, NINscan by itself can collect data continuously and independently for more than 24 h. NINscan data collection does not need a central receiver (computer) to support the data collection, such as those required by wireless communication-based aNIRS devices. This way the total weight of the devices required for data collection is reduced (NINscan 4 with batteries weighs only 170 g), and there is less restriction to the range of activities (without distance restrictions such as needed for reliable wireless communication-based aNIRS monitoring). This is especially important for monitoring in extreme environments, such as in the study of mountain sickness and space applications. Second, NINscan 4 provides multimodality monitoring capabilities, including three actigraphy channels (x, y, and z accelerations) and one ECG channel are recorded together with the systemic and cerebral hemodynamic channels; all channels are strictly synchronized.

In this article, using battery-powered NINscan 4, we performed simultaneous and continuous monitoring of cerebral hemodynamics, systemic hemodynamics, ECG, and actigraphy for 24 h, at 250-Hz sampling rate. Subjects were asked to keep a voice or written log of their activities throughout the day, and the two integrated event buttons were utilized by subjects to mark special events. The timing of the event button press was recorded to help precisely identify the events of interest.

To monitor cerebral and systemic hemodynamics, four aNIRS channels were implemented. A dual wavelength (785 and 830 nm) laser diode was used as the light source (Axcel Photonics, Inc., Marlborough, Massachusetts), and two OPT101 photodiodes (Texas Instruments, Inc., Dallas, Texas) were used as detectors. Laser power at each wavelength was about 3.5 mW, under the maximum permissible exposure (MPE) standards for skin illumination (The skin MPE is about 300 mW/cm^2 for NIR light, depending on the wavelengths; and NINscan illumination intensity is about 30 mW/cm^2). An optical diffuser was used to expand the laser beam profile and reduce spatial density of the light. The systemic hemodynamics was acquired from a source–detector pair with 1.5-cm separation, whereas the cerebral hemodynamics was acquired from source–detector pair at 4.0-cm separation. We will refer to measurements from short source–detector pair or the scalp/skull hemodynamics as "systemic" because it is not regulated, as a comparison to the regulated cerebral hemodynamics. Precisely speaking, it is only a local estimate of the systemic hemodynamics. The four aNIRS channels were implemented using frequency division multiplexing and lock-in demodulation scheme, with a signal detection bandwidth of 20 Hz. A three-dimensional (3-D) accelerometer, ADXL325 (Analog Devices, Inc., Norwood, Massachusetts), was used as the sensor for NINscan 4 body position/orientation and actigraphy measurements. The accelerometer was sensitive to both static acceleration of gravity (e.g., tilting), as well as dynamic acceleration, resulting from motion, shock, or vibration. The accelerometry channels measured acceleration in x, y, and z directions up to $+/-5$ g, with a bandwidth of 40 Hz. The single ECG

channel utilized the standards for regular ECG Holter monitoring, with a bandwidth of 0.1 to 40 Hz; and disposable Ag-AgCl ECG electrodes were used for ECG monitoring.

Successful long-term aNIRS recording in people's real life activities depends critically on the system's resistance to motion artifact; therefore, it is also worth mentioning the motion resistance features of NINscan system. In NINscan 4, many measures to improve the systems resistant to motion artifact were included in the design. Motion recording-based adaptive filtering algorithm have been shown to reduce motion artifacts;[39] our tests suggest that both simultaneous recording of subjects' motion signal and the multidistance optical probe helps with the identification, reduction, and management of motion artifacts during NINscan monitoring. In our NINscan probe, there are four optical channels, the short source–detector distance channels are used for monitoring of systemic hemodynamics, and the far source–detector channels are used to monitor cerebral hemodynamics. Usually motion artifacts appear in both near and far optical channels, and this "common mode" feature of motion artifact can be used for motion artifact identification. With a multidistance optical probe, we can also apply scalp/skull interference correction in our data analysis to acquire higher sensitivity and specificity in brain function measurements.[40–44] Other details of motion artifact resistant probe and system design have previously been reported.[24] These include soft and light weight probe design, with flexible curvature adapted to the of the shape of the head; adhesive probe surface to secure the probe's position relative to the skin, and reduce the possibility of probe shifting; elimination of any sharp edges or pressure-points and appropriate attachment of the probe to the head to ensure subjects' comfort. Since the laser diode is integrated directly on the probe, it is important that the diode has efficient heat dispensing structure. With prolonged monitoring time, what are minor issues for short-term measures, such as the pressure of the probe or temperature of laser diodes, become critical and need to be carefully managed to ensure subjects' safety and comfort. For long-term probe attachment, it is also important that the probe be made of medical grade and skin friendly materials to reduce possible skin irritation.

3.2 *Human Subject Data Collection*

The experimental protocol was approved by the MGH IRB and data were collected from healthy subjects. The optical probe was secured via its adhesive surface and the head band over the right prefrontal cortex (between 10/20 position F_4 and F_{p2}, or approximately Brodmann areas 10 and 46). The reasons we choose to monitor prefrontal cortex in our feasibility tests is because the area is important in attention, working memory,[45] decision making,[46] and sleep-affected neurophysiologic processes,[47] and that it is easy to attach the probe and acquire good signal quality on the forehead. ECG was collected from chest leads. The motion sensor was attached to the optical probe on the head. The recorder was carried in the subject's pocket or a separate small bag, as was convenient.

At the beginning of the recording, an event button integrated in the NINscan 4 box was pressed at a specific time on the subjects' watch, which was used to keep the activity log. This way the NINscan recording time and the diary time could be synchronized. Subjects were asked to press event buttons to record the beginnings and ends of consecutive activities during the entire data collection period. Event marker presses were accompanied by verbal entries recorded through a voice recorder, which were subsequently compiled into an auditory data activities log used in data preparation and analysis.

Few restrictions were placed on the subjects' activities during the 24-h recording. The most significant one was to avoid getting the NINscan device wet (e.g., bathing). Two data collection examples are shown in Fig. 1.

3.3 *Data Analysis*

For aNIRS channels, the raw 250-Hz optical data were corrected for dark current and digitally low pass filtered at 5 Hz (in addition to the instrument filter). To acquire the total hemoglobin

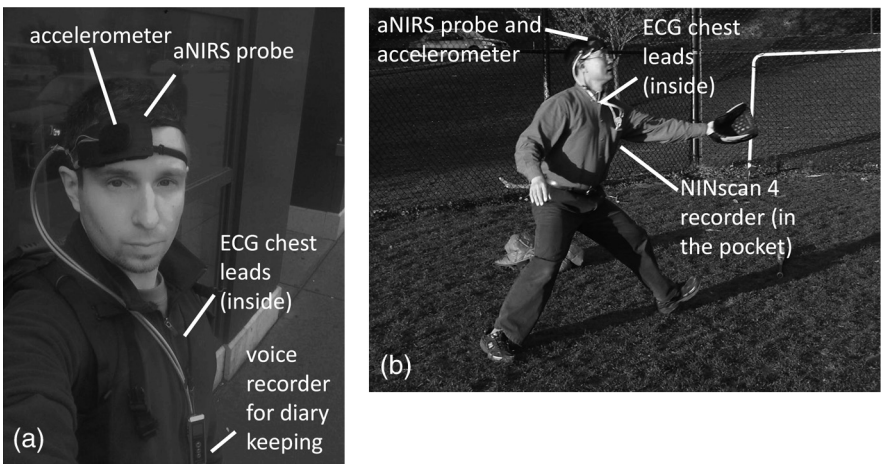

Fig. 1 Examples of 24-h ambulatory recording of cerebral hemodynamics, systemic hemodynamics, ECG, and actigraphy during subjects' daily activities. (A) Monitoring of a subject before he went on the subway. For this subject, the optical ambulatory near infrared spectroscopy (aNIRS) probe and the accelerometer were located on the right side of the forehead. This subject used a voice recorder (together with the event buttons) to log events during his daily activities. The NINscan 4 recorder was in his pocket (not shown in the picture). (B) Monitoring of a subject while he was playing baseball in the field. The aNIRS probe and the accelerometer were again placed on the right side of the subjects forehead, and the NINscan 4 device was conveniently put in his shirt pocket. For both subjects, ambulatory ECG was simultaneously recorded using standard chest leads.

(HbT) and oxygen saturation (Sat) levels, we first calculated the optical density changes (delta OD) from raw aNIRS measurements. This was done by normalizing the 24-h raw datasets with the averaged data collected during earliest morning 0:00 to 0:30 a.m. in that dataset (defined as the "baseline" for this test). Combining the multidistance aNIRS measurements, the interference from the superficial layers (e.g., scalp and skull) were estimated and removed from cerebral hemodynamics calculation similar to previous approaches.[40–44] The deoxy-hemoglobin (Hb) and oxy-hemoglobin (HbO_2) concentration changes (compared with the 0:00 to 0:30 a.m. baseline section) were calculated using modified Beer–Lambert law[48,49] and layered tissue model;[40,44] and then the total hemoglobin concentration (HbT) change and tissue oxygen saturation (Sat) are calculated:

$$[\delta \mathrm{HbT}] = [\delta \mathrm{Hb}] + [\delta \mathrm{HbO_2}], \tag{1}$$

$$\mathrm{Sat} = \frac{[\delta \mathrm{HbO_2}] + [\mathrm{HbO2_0}]}{[\mathrm{Hb_0}] + [\delta \mathrm{Hb}] + [\mathrm{HbO2_0}] + [\delta \mathrm{HbO_2}]}. \tag{2}$$

Here, $[\delta \mathrm{Hb}]$ and $[\delta \mathrm{HbO_2}]$ are the concentration changes of Hb and HbO_2, $[\delta \mathrm{HbT}]$ is the concentration change of the total hemoglobin, Sat is the oxygenation level, and $[\mathrm{Hb_0}]$ and $[\mathrm{HbO2_0}]$ are the averaged (or baseline) Hb and HbO_2 concentrations. Since NINscan uses continuous wave NIRS techniques, it provides measurements of the change of HbO_2 and Hb concentrations only, therefore the oxygen saturation level was calculated based on estimated tissue concentrations: $[\mathrm{Hb_0}] = 18\ \mu\mathrm{Mol}$ and $[\mathrm{HbO2_0}] = 41\ \mu\mathrm{Mol}$. These baseline concentrations were estimated based on the literatures[43,50] as well as our radio frequency NIRS measurements.

For ECG analysis, the QRS detection and heart rate estimation were performed based on the traditional Hamilton algorithm,[51] available from Physionet.org. Median filtering over 5 heart beats was used to smooth the final heart rate.

For actigraphy analysis, the raw accelerometer readings were converted to gravity units (g values). The orientation and position of the accelerometer were recorded, so the correct x (left–right), y (posterior–anterior), and z (inferior–superior) directions could be identified. Therefore, both body position and movement of the subject's head could be measured. To estimate the activity level, we use the digital integration method to calculate an "activity score:"[26] the amplitude of the total acceleration (combined acceleration from x, y, and z axes) was band-pass filtered to 0.25 to 3 Hz, then integrated using a time window of 2 s. An actigraphy-based algorithm can be used to automatically distinguish sleep episodes from wakefulness. Previous work[27,28] shows that this algorithm can correctly distinguish sleep from wakefulness ~90% of the time, as compared with the gold standard polysomnography. Since our accelerometer was placed on the head instead of the wrist (as most commercial actigraphy meters do), and that the coefficients and thresholds used in commercial products to distinguish sleep and wakefulness are proprietary, we set up our own parameters. In the equation to calculate D and identify sleep and wakefulness,[27,28] we set $P = 0.13$; $W_{-4} \sim W_{+2}$ to be 0.010, 0.015, 0.028, 0.031, 0.085, 0.015, and 0.010, respectively; and $D < 0.00055$ indicates sleep.

As a simultaneously monitored auxiliary parameter, accelerometer data (from which actigraphy is derived) provides the following information: (1) quantitation of activity and movement; (2) identification of motion artifacts for data analysis and potential correction;[39] (3) subjects' body position (e.g., stand, lying down supine), as blood distribution and even tissue status may vary as body position changes, therefore, it is important to use body position as a reference while explore tissue hemodynamics and activity; and (4) help substantiate a log of activities. Actigraphy, together with NINscan 4 event buttons and manual/verbal logs, serves as a good "diary" keeping and checking tool, allowing us to easily identify different types and timings of real life daily activities, such as sleep, work, sports, riding elevators, and even driving.

To reduce the temporal correlation of the measurements in our time series, we down sampled the time series before the statistical analysis. For example, in our long-term circadian study, where the signal was filtered to 0.005 Hz, before linear regression we reduced the number of measurements to 200 s/sample, or 438 data points per one 24-h time series. Linear regression analysis was conducted, with significance identified by $p < 0.05$.

4 Example Continuous 24-h Recording

The amount of data collected during a single 24-h recording of cerebral hemodynamics, systemic hemodynamics, ECG, and actigraphy during daily activity was ~350 MB (uncompressed). Here, we first present the raw data from a typical 24-h test, and then discuss with experimental results how we manage the motion artifacts, a key technical challenge in ambulatory monitoring.

4.1 *Raw 24-h Recording Data*

An example 24-h raw dataset is shown in Fig. 2. In this recording, data collection was initiated at 11:26 a.m. on day 1, and completed at 11:46 a.m. on day 2. During the 24-h data collection period, the subject participated in his normal daily activities, including miscellaneous static and dynamic tasks at home, preparing food, eating, daily hygiene, socialization with family members and coworkers, commute to and from work using public transport (subway and shuttle bus), resting, yawning, falling asleep, and sleeping. During the night, the subject slept with minor interruptions. All signals in Fig. 2 are plotted as raw digitization units (A/D range = 0 to 4096), and the rows in each subfigure are motion (actigraphy), ECG, and aNIRS recordings, respectively.

Figure 2(a) is an overview of the whole 24-h recording. The 24-h overview is usually used to ensure the overall signal quality, and to identify possible low quality segments such as those from signal saturation or sensor detachment (neither of these were detected). From the accelerometer recording, we can clearly identify the body position and activity level change during the day and during the night. From the amplitude range, we can tell that the ECG recordings are high quality, with occasional artifacts due to motion. The aNIRS signals exhibited no saturation, signal drop-out, or other unexpected features. During the 24 h recording, the subject pressed the two event buttons 80 times, the timings of which, labeled as E1 or E2, were all precisely logged into the memory and shown in this figure. Together with the subjects' detailed diary, different events, and activities can be accurately identified, and their associated body positions, movements, ECG, systemic, and cerebral responses can be calculated.

Figure 2(b) expands 1 h of the recording [the segment in yellow in Fig. 2(a)] following one of the event button presses in the evening. The associated diary for this event button press read: "Got up from the low arm chair, walked to the kitchen with the computer, sat in the high-back chair, continued working on the computer". The three-axis accelerometry recordings demonstrated the body position change associated with this "sat in

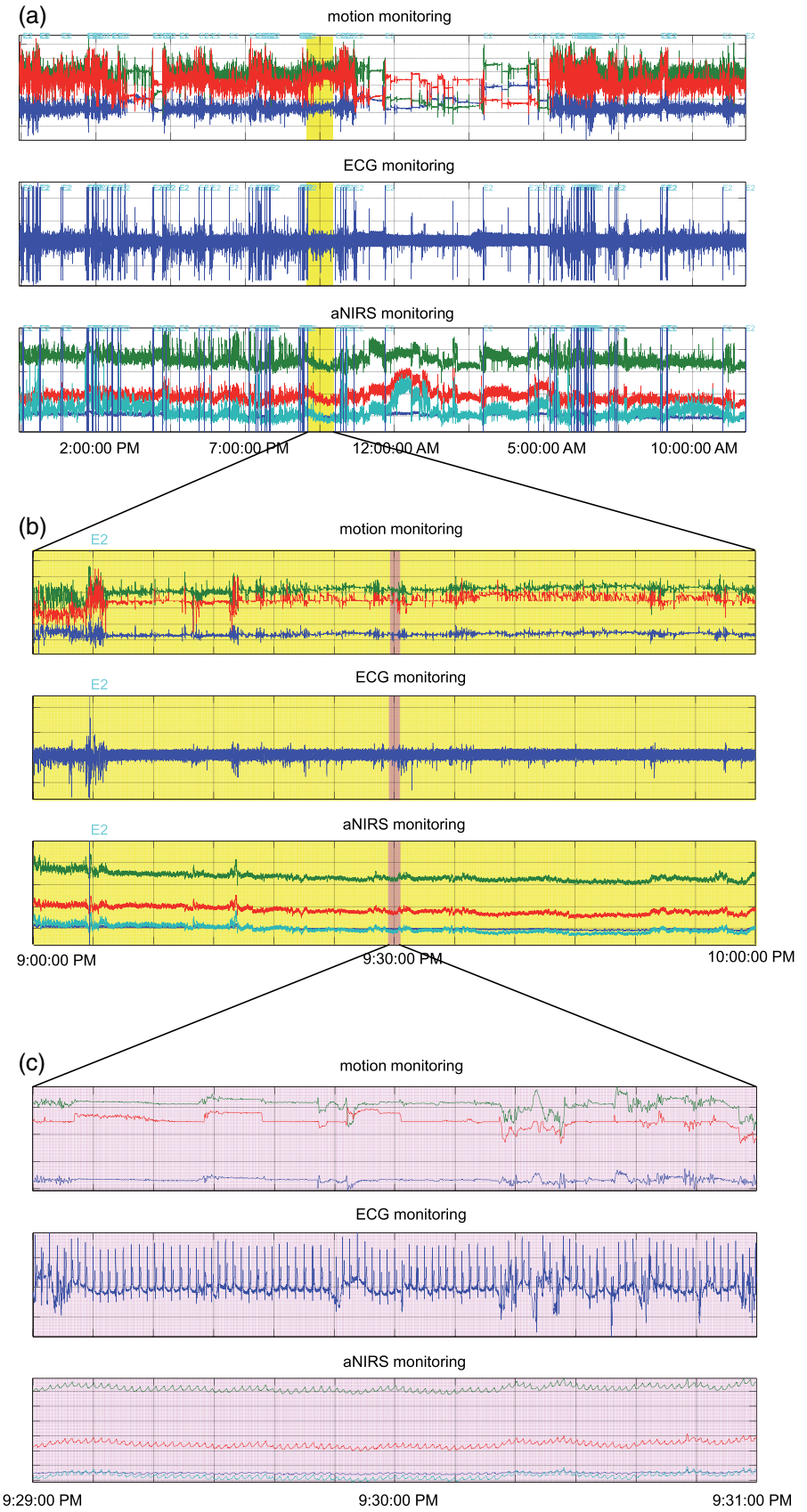

Fig. 2 An example 24-h multimodality NINscan 4 monitoring dataset. (A) 24-h overview of actigraphy, ECG, and aNIRS raw data. This dataset demonstrates good signal quality, and we can clearly see (from actigraphy) the activity level change between awake and sleep periods. The timings of event button press were all logged to the millisecond. (B) View of a 1-h raw data before and after pressing an event button. The diary indicated the subject was working on the computer after pressing the event button. (C) View of 2-min raw data to demonstrate in detail the bandwidth and quality of the raw recordings.

the high-back chair" event, and the subject's body position remained stable after that, with occasional small movements. The ECG recordings and aNIRS recordings were stable through this period as well.

Given the high-resolution recorded data, even the zoomed Fig. 2(b) only shows the amplitude range and low-frequency trend in signal variations. In Fig. 2(c), the curves were further zoomed to show 2 min of data [the segment in pink in Fig. 2(b)] in detail. In this subfigure, we can clearly see the individual heart beats in ECG and aNIRS, which demonstrate the bandwidth and high quality of the raw recordings. From these data, aNIRS channels in NINscan 4 appear more motion resistant than ambulatory ECG recordings. This can be verified by comparing the motion, ECG and aNIRS signal in Fig. 2(c).

4.2 *Motion Resistance of NINscan 4 Recordings*

To further demonstrate the motion resistant features of NINscan 4, we examined the influence of head motion in our aNIRS recordings, and compared it with the subject's spontaneous and physiological signal variation levels.

During one of our 24-h ambulatory recordings, the subject was asked to rapidly shake his head "no" (moving from left to right, and then back). After completing the recording, we compared the subject's systemic hemodynamic measurements (calculated from aNIRS channels with source–detector separation of 1.5 cm) during the head movement with the spontaneous signal variations during his motionless sleep in the night.

Figure 3 shows the result. Column A is the episode of the recordings when the subject was sleeping. In this ~2-min recording, the subject was in a laying-down position, facing left. In the first row in column A, the total acceleration (combined acceleration from all three directions) indicates that the subject was very still, with no obvious movement (<0.02 g). From the systemic hemodynamic recording (second row), we can see that the amplitude of cardiac activity in [δHbT] was about 3 μM. A spontaneous low-frequency fluctuation can be identified, with a valley at 03:35:20 a.m. and a magnitude of -12 μM. Column B shows the result when the subject rapidly shook his head. The first row of column B demonstrates that this intentional head movement introduced a total acceleration of ~1 g (on top of the 1-g gravity level). The aNIRS recordings, however, were essentially unaffected by this motion. The major hemodynamic variation is still the cardiac activity, which is totally out-of-phase with the head movement; and the magnitude of the cardiac activity (about 3 μM) did not change during the activity as compared with no head movement at the beginning and end of this period.

For both the sleep and the head movement data segments, we further plot the hemodynamic variation as a function of the head acceleration (third row in Fig. 3). For linear regression analysis, the range of the [δHbT] and the total acceleration were first

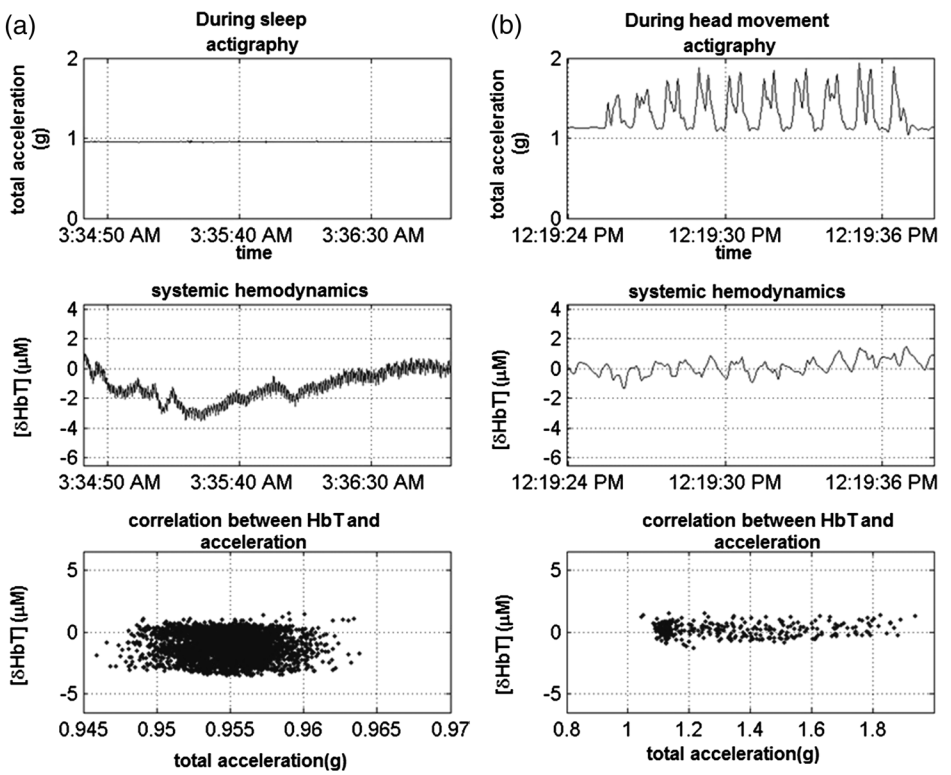

Fig. 3 Tests for NINscan 4 motion resistance. Column A: One segment of NINscan 4 recordings during sleep, which demonstrated the level of physiological signal variation. The total acceleration recordings (row 1) showed that subject had little movement during sleep; the systemic hemodynamics (row 2) showed the subject's physiological variations (cardiac about 1 mM, slow wave about 6 mM). The linear regression analysis showed no correlation between hemodynamic variations and motion. Column B: NINscan 4 recordings while the subject was shaking his head. The adhesive probe was secured on the right side of the subject's forehead. The accelerometry recordings showed the subject's total acceleration was up to 1 g, the systemic hemodynamics measurements did not show obvious motion artifacts (row 1) corresponding to the head movement; the major variation in the signal was from cardiac activity. Again linear regression analysis showed no correlation between hemodynamic variations and motion.

normalized to range of 0 to 1, and the signals were down sampled to 5-Hz sampling rate to reduce temporal autocorrelation and improve the independence of separate measurements. For the sleep data section, the linear regression of [δHbT] versus total acceleration gave Pearson correlation coefficient of $r = -0.07$ (slope $= -0.09$; $p > 0.05$); for the head shaking data section the regression gave Pearson correlation coefficient of $r = 0.01$ (slope $= 0.01$; $p > 0.5$). Therefore, acceleration from both vigorous head movement ($\sim 1\ g$) or sleep ($\sim 0.02\ g$) demonstrated no significant change in the hemoglobin measurements in aNIRS; compared with the cardiac and other spontaneous physiological hemodynamic variations in the long-term recordings, artifacts introduced by head motion were minor and could be ignored.

5 Experimental Demonstration of the Unique Capabilities of Multimodality Long-Term Ambulatory Brain Function Recordings

NINscan 4 recoding features several unique advantages, including its long-term data collection and analysis capability, capability of catching transient events with unpredictable happening onsets, capability of measurements during daily activity in the real world, and simultaneous multiparameter data analysis. In this section, we demonstrate those features using typical experimental data.

5.1 *Application of NINscan 4 Recordings in Circadian Study*

Comparison of physiological or pathological features during wakefulness and during sleep is key to the study of people's circadian physiology. For example, it is well known that during sleep, due to reduced physical activity of the human body, subjects will demonstrate lower heart rate and overall metabolism level. Circadian brain physiology is of considerable interest but—while many technologies have been applied, such as ECG, electroencephalography (EEG), fMRI in the study of sleep and circadian cycles—so far no existing technology has been able to continuously monitor and compare cerebral hemodynamic features through a 24-h cycle.

Using NINscan monitoring, we are able to compare the cerebral hemodynamic features during wakefulness (normal daily activities) and during sleep. Figure 4 shows a typical result comparing the average cerebral blood volume during daily activities and during sleep (at the subject's home). Again, the NINscan probe was located on the forehead over the right frontal cortex, and cerebral hemodynamics, systemic hemodynamics and three axis accelerometries were all performed on this region. In order to clearly demonstrate the low-frequency trend in the circadian features, we low pass filtered the signals with a cutoff frequency of 0.005 Hz. The result is shown in Fig. 4 and Table 1.

Figure 4(a) shows the change in activity level across a full day. It is clear that during the night the activity score was significantly reduced. From Table 1, we see that during wakefulness the average activity score was 0.0092, while during sleep it was 0.0001, more than 90-fold reduction. Here, the wakefulness and sleep were identified using the actigraphy algorithm. The variations in activity level and the heart rate [Fig. 4(b)], derived from ECG, were closely aligned during wakefulness (linear regression on data down sampled to one measurement ever 200 s; $r = 0.78$, $p \ll 0.0001$). Average heart rate during sleep in this subject was 43 bpm, 20% less than the heart rate during the day, and the heart rate decrease is significant ($p \ll 0.05$). This overall low resting heart rate was confirmed by both NIRS and ECG using independent instruments.

Although reduced activity level and heart rate during sleep is expected, changes in the cerebral blood volume level [Fig. 4(c)] and oxygenation level [Fig. 4(d)] during sleep compared with wakefulness have not to our knowledge been experimentally studied. In this single case, we compared the blood volume level and oxygenation level during sleep and wakefulness to demonstrate the feasibility of this analysis based on long-term data collection. Our results show that [δHbT] (HbT change compared with the baseline level measured at 12:00 to 12:30

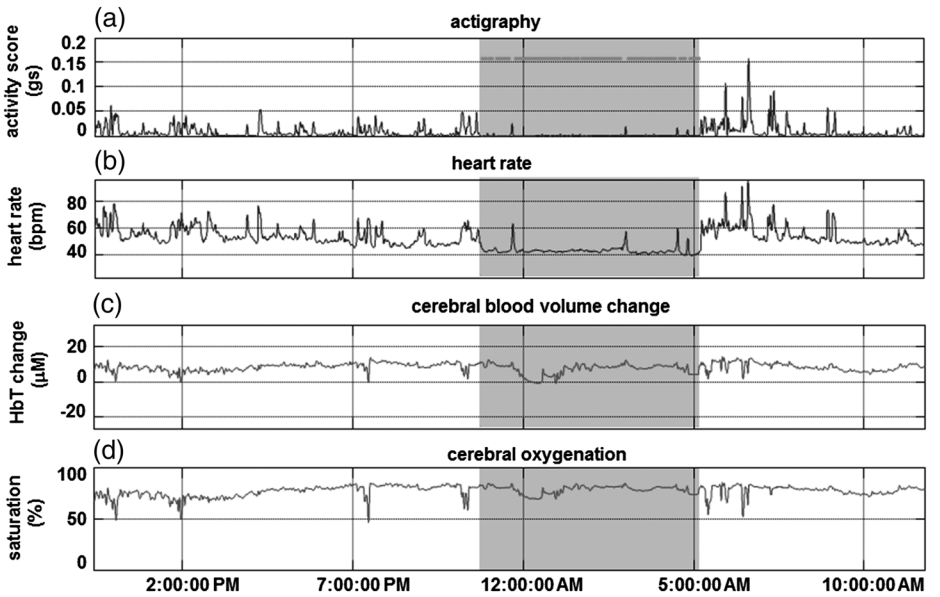

Fig. 4 Application of multimodality NINscan 4 monitoring in circadian studies: comparison of actigraphy (A), heart rate derived from ECG (B), cerebral hemodynamics including total hemoglobin concentration change (C), and oxygenation change (D) during wakefulness and sleep. The shadowed section indicates the bedtime logged on the subject's diary; the line segments in the actigraphy indicate the sleep time detected using actigraphy-based algorithm.

Table 1 Application of multimodality NINscan 4 monitoring in circadian studies: comparison of actigraphy, heart rate, cerebral hemodynamics during wakefulness and sleep.

	Activity score	Heart rate(bpm)	Cerebral blood volume change (μM)	Cerebral oxygenation (%)
Wakefulness	0.0092 (0.015)	54. 1 (7.4)	8.7 (2.2)	77 (5.3)
Sleep	0.0001 (0.002)	42.3 (1.2)	6.9 (3.3)	78 (3.9)
Difference (%)	−99%	−22%	−21%	1.2%
*P*value	4×10^{-9}	$<1\times10^{-20}$	2×10^{-10}	0.94
Change	Reduction	Reduction	Reduction	Not significant

a.m.) was $8.7+/-2.2$ μM during wakefulness, and $6.9+/-3.3$ μM during sleep. This represents a significant 21% reduction in [δHbT] ($p \ll 0.0001$). The cerebral oxygenation level change, in contrast, was not significant, being estimated at $77\%+/-5.3\%$ during wakefulness and $78+/-3.9\%$ during sleep ($p > 0.05$). Tissue oxygen saturation level should lie between the arterial oxygen saturation and venous oxygen saturation; it is an averaged value for blood contained in all arteries, arterioles, capillaries, venules, and veins in the area probed by the photons (related to the diffuse light sensitivity profile). It has been shown that sleep cerebral metabolic rates of glucose and oxygen decrease by 44% and 25%, respectively, during specific phases of sleep.[52,53] When further assuming a stable oxygen extraction rate, the static cerebral oxygenation would suggest a reduced blood volume, as measured.

NINscan provides a unique opportunity to measure and compare parameters estimated from long duration measurements and during daily activity. Sleep is widely studied using NIRS,[47,54–59] however, most of the previous studies were performed with short term tests (e.g., afternoon nap) or sleep in the lab environment. The result presented here demonstrates the long-term data acquisition and analysis capability of the NINscan monitoring, and to the best of our knowledge, is the first to extend the experimental study of cerebral hemodynamics during wakefulness and sleep during a full 24-h period of unrestricted activity. This will enable, for example, detailed investigation of circadian influences on cerebral physiology.

5.2 *Unpredictable Symptom Capture: Response to Environmental Noise during Sleep*

Many physiological or pathological conditions—syncope, epilepsy, schizophrenia, hot flashes, delayed stroke—feature transient symptoms with unpredictable onsets. Detecting such conditions requires long-term ambulatory recording to increase the opportunity catching such unpredictable events. Here, we present an interesting nonclinical example NINscan 4 recording of a subject who woke up unexpectedly to environmental noise.

The unexpected awakening event happened in the early morning when the subject was in motionless sleep. The subject was suddenly awoken by environmental noise. He raised his head, determined what was happening, pressed the event button, then went back to sleep. The subject recalls the event being quite short: he felt that he "immediately" woke up at the environmental noise and from his being aware of the noise to his going back to sleep; the whole process was estimated to take 1 to 2 min.

The event as captured by NINscan 4 monitoring is shown in Fig. 5. The four rows in the figure are A, three axis acceleration (bandwidth 0 to 5 Hz); B, heart rate (derived from ECG, 5 heart beat median filtered); C, blood volume change (bandwidth 0 to 5 Hz) and D, oxygenation change (bandwidth 0 to 5 Hz), respectively.

The event button was pressed at 4:30 a.m., and we can clearly see motion, heart rate and cerebral blood volume, and oxygen saturation change before, during, and after this event. From the motion channels, we can see that the subject was in his supine position (blue, green, and red indicates x, y, and z directions, where y is points up with magnitude of 0.75 g), and remained very still until 4:26 a.m., where he showed two slight movements. The subject then woke up at 4:30 a.m., and demonstrated substantial head motion. He lay down again, with slight body position change. After 4:34 a.m., the subject was motionless again.

What is interesting in the recordings is that the subject recalled this event being very short, and he felt that he slept very well both before and after this short event (in Fig. 5, we marked the section where the subject felt conscious with yellow background). However, the recordings of heart rate, cerebral blood volume, and oxygenation all demonstrate changes several minutes "before" the subject felt conscious. The subject's heart rate was about 41 during sleep, at 4:26 a.m. his heart rate demonstrated significant increase (up to 60 bpm) and fluctuation, along with enhanced cerebral hemodynamic fluctuations, although he was not physically moving (as indicated by the mostly silence in the 3-D accelerometer recordings). His response to the environmental noise, shown as elevated heart rate, cerebral blood volume, and oxygenation (both in magnitude and dynamic fluctuation) continue, without him being conscious of the environmental noise, until the point when he felt that he woke up and begun to move (4:30 a.m.). All the parameters were further elevated and peaked at 4:30:50 a.m., where the heart rate went up to 78. After 4:34 a.m., all parameters quickly went back to the regular sleep level. The consequences of environmental noise on the recorded physiology were very consistent: almost all parameters including heart rate, cerebral and systemic hemodynamics show coincident variations.

The horizontal green bar in the actigraphy recording is the sleep section identified by the actigraphy-based sleep/wakefulness identification algorithm. Although not as early as the elevation of heart rate and hemodynamic level, the beginning of the episode of "wakefulness" identified using the actigraphy-based algorithm (4:28 a.m.) is also earlier than the subjective feeling described by the subject.

This example demonstrates an interesting and fairly large difference between the "objective measurements" and the "subjective feeling," which is important in many social or psychiatric studies. It also demonstrate that with long-term ambulatory monitoring techniques it is possible to record objective physiological or pathological parameters leading, during, and following a specific and unpredictable event; the data collection procedure and the data analysis for the "unexpected sudden wakeup" example presented here is not only relevant to sleep studies, but also for catching and analyzing symptoms such as epilepsy, syncope, and others. We expect NINscan 4 to be a powerful tool to understand the conditions that lead to

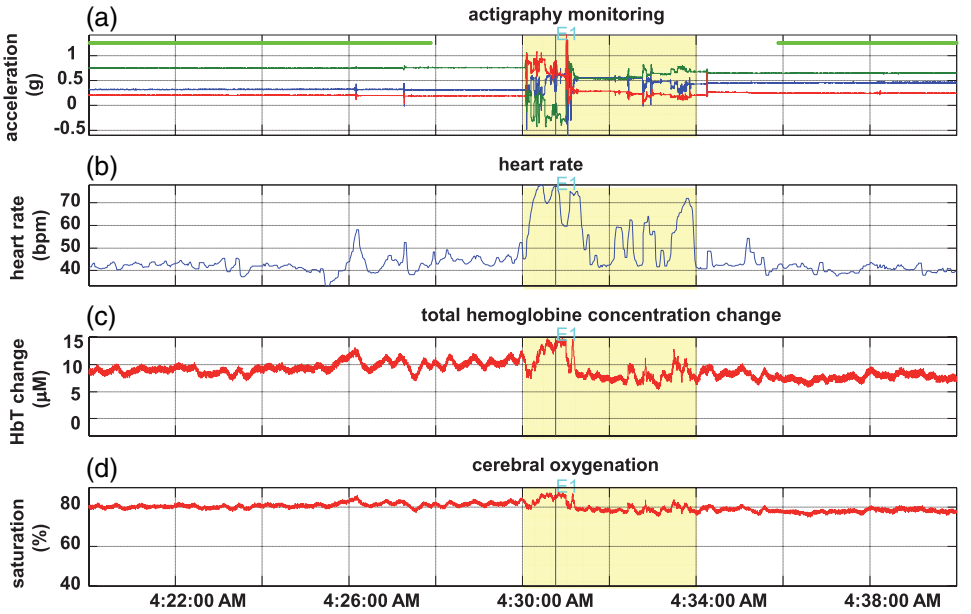

Fig. 5 Example of NINscan 4 recording of a transient event with unpredictable onset. In this segment of data, the subject was woken up unexpectedly by environmental noise. The E1 event button was pressed by the subject upon awakening, and from the NINscan 4 recording we can clearly see the (A) actigraphy, (B) heart rate derived from ECG, (C) cerebral total hemoglobin concentration change, and (D) cerebral oxygen saturation before, during and after this unexpected event. The horizontal green bar in the actigraphy recording is the sleep section identified by the actigraphy-based sleep/wakefulness identification algorithm.

those symptoms, the features of the events, and their consequences measured in cerebral and systemic perfusions and oxygenation.

6 Discussion

ANIRS provides long-term cerebral hemodynamic measurements based on diffused NIR light and spectroscopy analysis and it makes long-term monitoring of systemic and cerebral hemodynamics possible during daily activities. The unique technical advantages of aNIRS include its capability to catch transient events, high-temporal resolution, good specificity, portability, and low cost. ANIRS provides new potential for the diagnosis and management of the above mentioned diseases or academic studies, both as an independent tool, or as a supplementary modality to currently used standard diagnosis.

Some important human physiology, pathology, or cognitive-behavioral studies are based on observations and measurements of a subject over many hours or even days. Sleep physiology and sleep disorders, circadian rhythms (e.g., wakefulness and sleep patterns), circadian transitions, cognitive-behavioral performance associated with sleep restriction, and deprivation, are all good examples. In the past, in-depth and quantitative understanding of the long-term human physiology or pathology has depended on prolonged measurements using modalities such as EEG, ECG, blood pressure, and actigraphy. For example, much of our current understanding of neurophysiologic mechanisms associated with wakefulness and sleep stems from EEG studies;[60] and wakefulness and different stages of sleep are described using featured EEG patterns.

Long-term cerebral and systemic hemodynamics, based on aNIRS technology, provides a separate dimension for the understanding of the above mentioned studies. The advantages of this new method are (1) similar to fMRI, the blood supply and oxygen consumption information acquired from aNIRS is a relatively direct measurement of cerebral and systemic metabolism; and (2) aNIRS provides local measurements, only tissue within the optical probing area is measured, therefore the spatial specificity is higher. As a comparison, the origins of the non-invasive EEG measurements in many cases are difficult to reconstruct due to the volume conduction effect in the human head.

Using our long-term ambulatory and multimodality NINscan 4 monitor, we successfully performed continuous 24-h recordings of cerebral and systemic hemodynamics, ECG, and actigraphy on subjects during daily activities in real life. We demonstrated NINscan4's motion resistant features, and presented experimental results demonstrating stable, long-term multimodal data collection. This opens the door to 24-h circadian brain physiology assessment, provides a new approach for symptom capture studies, and facilitates a wide range of new studies and experimental designs. To the best of our knowledge, it is the first report of such recordings.

Based on this work, we were able to compare cerebral blood volume and oxygenation changes during sleep and wakefulness, and identify a subject's systemic and cerebral response to environmental noise before, during and after environmental noise during sleep. Being case studies, no conclusions can be drawn but initial (testable) hypotheses can be formulated. For example, our preliminary findings suggest decreased cerebral perfusion during normal sleep, no change in cerebral oxygenation, and the ability to affect such variables with at least auditory stimuli during sleep. However, our primary the goal was to demonstrate the feasibility, unique capability and potential of our long-term ambulatory multimodality NINscan monitoring. Although there was insufficient space to report these in detail, we also found that various other activities in real daily life—including sports, meals, driving, yawning, and others—demonstrate consistent alterations in cerebral hemodynamics. Further

technology development and human subject tests are required to follow up such findings.

The 24-h monitoring that NINscan 4 enables can provide rich temporal and spectral details about systemic and cerebral hemodynamics variations as well as actigraphy and ECG. With such information, we can perform many in-depth, application-oriented analyses to reveal the hidden information. For example, we can perform component analysis or study signal variations in specific frequency bands and their temporal evolution, in relation to subject states (e.g., sleep-wake), sensory input (e.g., unexpected visual or auditory events), or specific activities (e.g., exercise, cognitive tasks). The multimodality capability of NINscan 4 provides us opportunity to study the relationships between different modalities. Such multimodel data can help develop more complete models of human hemodynamics and how such physiology evolves over time.

NINscan 4 is a fourth-generation wearable monitoring device and as such incorporates the experience accumulated over the past 7 years of NINscan technology development. Although providing novel capabilities, NINscan 4 nevertheless has its limitations. First, it can only monitor one cerebral location; in many applications, larger spatial coverage of the brain and simultaneous EEG are often preferred. Second, NINscan 4 data acquisition and analysis is currently based on postprocessing similar to ECG Holter home monitoring—data is collected and stored for analysis after data collection. In some applications, however, real-time display of the aNIRS and auxiliary measurements are preferred. Third, thus far our NINscan 4 cerebral monitoring has focused on prefrontal and frontal lobes. This partly is because there is less hair on the forehead, which enables adhesive securing of the optical probe. Although these represent real limitations, NINscan 4 still has broad applicability and we are simultaneously developing solutions each of these limitations.

We have demonstrated experimentally that NINscan 4's motion artifact at 1-g head movement is smaller than physiological hemodynamic fluctuations during motionless sleep. From our experience, head movement by itself is not a significant artifact generator; however, artifacts could be generated by physically pressing on, stretching or repositioning of the optical sensor. Because of our lightweight, motion resistant probe and system design and the fact that the probe is adhered to the skin, the head movements usually have little effect on the relative position of the probe. However, probe pressure or position could change, for example, when the subject heavily frowns, or lies down a certain way (e.g., on his stomach) with his head probe pushed or stretched by the pillow; and aNIRS signal will change consequently.

To reduce these types of artifacts, we have minimized the chance of motion artifacts while sleeping via our probe design. Also, because the probe is adhered to the forehead, the probe will typically return to its original position when the temporary external forces disappear, given the elasticity of the skin. Furthermore, with the help from the accelerometer recordings, the probe stretching or repositioning related artifacts can be identified using following criteria: (1) the onset and duration of the variation in hemodynamic channels and body position change aligns well; and (2) the artifact appears in all optical channels (near and far source–detector separations and both wavelengths)—a common mode variation. This is because both the far and near detectors share the same optical sources, and the two wavelengths are implemented in the same laser diode. If probe repositioning happens, for short-term data analysis, we can treat the stable section (indicated by the motion sensor) after the probe repositioning as measurements with a new baseline; for long-term data analysis, since usually the probe will go back to the original position due to skin elasticity, the probe repositioning artifact can be smoothed out. If signal variation occurs when there is no obvious motion, or signals from different source–detector pairs demonstrate different types or shapes of variation, with no obvious correlation with the motion recordings, we can tell the signal is not contaminated by artifact.

We expect NINscan 4 will provide physiological and pathological information about brain function in experimental contexts that have previously been impossible to investigate. We hope such monitoring technology can be developed into independent or adjuvant diagnosis tool and demonstrated to be clinically useful in (1) the prevention, diagnosis and management of many diseases with low frequency and transient cerebral symptoms (2) the long-term applications such as sleep and circadian studies, as well as (3) remote, low-resource, underserved, and even extreme settings such as environmental and space medicine.

Acknowledgments

This work was supported by the National Space Biomedical Research Institute through NASA NCC 9-58.

References

1. J. K. Chen et al., "Functional abnormalities in symptomatic concussed athletes: an fMRI study," *NeuroImage* **22**(1), 68–82 (2004).
2. J. M. Stern, "Simultaneous electroencephalography and functional magnetic resonance imaging applied to epilepsy," *Epilepsy Behav. E&B* **8**(4), 683–692 (2006).
3. C. Altamura et al., "The longitudinal changes of BOLD response and cerebral hemodynamics from acute to subacute stroke. A fMRI and TCD study," *BMC Neuroscience* **10**, 151 (2009).
4. M. E. Zimmerman and M. S. Aloia, "A review of neuroimaging in obstructive sleep apnea," *J. Clin. Sleep Med* **2**(4), 461–471 (2006).
5. P. B. Fitzgerald et al., "An fMRI study of prefrontal brain activation during multiple tasks in patients with major depressive disorder," *Hum. Brain Mapp.* **29**(4), 490–501 (2008).
6. G. Strangman, D. A. Boas, and J. P. Sutton, "Non-invasive neuroimaging using near-infrared light," *Biol. Psychiatry* **52**(7), 679–693 (2002).
7. J. Blautzik et al., "Classifying fMRI-derived resting-state connectivity patterns according to their daily rhythmicity," *NeuroImage* **71**, 298–306 (2013).
8. C. M. Portas et al., "Auditory processing across the sleep-wake cycle: simultaneous EEG and fMRI monitoring in humans," *Neuron* **28**(3), 991–999 (2000).
9. M. Wolf, M. Ferrari, and V. Quaresima, "Progress of near-infrared spectroscopy and topography for brain and muscle clinical applications," *J. Biomed. Opt.* **12**(6), 062104 (2007).
10. M. Ferrari and V. Quaresima, "Near infrared brain and muscle oximetry: from the discovery to current applications," *J. Near Infrared Spectrosc.* **20**(1), 1–14 (2012).
11. M. Ferrari and V. Quaresima, "A brief review on the history of human functional near-infrared spectroscopy (fNIRS) development and fields of application," *NeuroImage* **63**(2), 921–935 (2012).
12. B. Chance et al., "Optical investigations of physiology: a study of intrinsic and extrinsic biomedical contrast," *Philos. Trans. R. Soc. London Ser. B-Biol. Sci.* **352**(1354), 707–716 (1997).
13. Q. Zhang et al., "Study of near infrared technology for intracranial hematoma detection," *J. Biomed. Opt.* **5**(2), 206–213 (2000).
14. T. Shiga et al., "Study of an algorithm based on model experiments and diffusion theory for a portable tissue oximeter," *J. Biomed. Opt.* **2**(2), 154–161 (1997).

15. H. O. Hisaeda et al., "Effect of local blood circulation and absolute torque on muscle endurance at two different knee-joint angles in humans," *Eur. J. Appl. Physiol.* **86**(1), 17–23 (2001).
16. Y. Hoshi, "Functional near-infrared optical imaging: Utility and limitations in human brain mapping," *Psychophysiology* **40**(4), 511–520 (2003).
17. T. Muehlemann, D. Haensse, and M. Wolf, "Wireless miniaturized in-vivo near infrared imaging," *Opt. Express* **16**(14), 10323–10330 (2008).
18. E. Lareau et al., "Multichannel wearable system dedicated for simultaneous electroencephalographynear-infrared spectroscopy real-time data acquisitions," *J. Biomed. Opt.* **16**(9), 096014 (2011).
19. S. K. Piper et al., "A wearable multi-channel fNIRS system for brain imaging in freely moving subjects," *NeuroImage* **85**(Part 1), 64–71 (2014).
20. M. Sawan et al., "Wireless recording systems: from noninvasive EEG-NIRS to invasive EEG devices," *IEEE Trans. Biomed. Circuits Syst.* **7**(2), 186–195 (2013).
21. M. Kiguchi et al., "Note: wearable near-infrared spectroscopy imager for haired region," *Rev. Sci. Instrum.* **83**(5), 056101 (2012).
22. H. Atsumori et al., "Noninvasive imaging of prefrontal activation during attention-demanding tasks performed while walking using a wearable optical topography system," *J. Biomed. Opt.* **15**(4), 046002 (2010).
23. M. L. Flexman et al., "A wireless handheld probe with spectrally constrained evolution strategies for diffuse optical imaging of tissue," *Rev. Sci. Instrum.* **83**(3), 033108 (2012).
24. Q. Zhang, X. Yan, and G. E. Strangman, "Development of motion resistant instrumentation for ambulatory near-infrared spectroscopy," *J. Biomed. Opt.* **16**(8), 087008 (2011).
25. F. Scholkmann et al., "A review on continuous wave functional near-infrared spectroscopy and imaging instrumentation and methodology," *Neuroimage* **85**(Part 1), 6–27 (2014).
26. S. Ancoli-Israel et al., "The role of actigraphy in the study of sleep and circadian rhythms," *Sleep* **26**(3), 342–392 (2003).
27. R. J. Cole et al., "Automatic sleep/wake identification from wrist activity," *Sleep* **15**(5), 461–469 (1992).
28. G. Jean-Louis et al., "Sleep detection with an accelerometer actigraph: comparisons with polysomnography," *Physiol. Behav.* **72**(1–2), 21–28 (2001).
29. M. Thorpy et al., "Practice parameters for the use of actigraphy in the clinical assessment of sleep disorders. American sleep disorders association," *Sleep* **18**(4), 285–287 (1995).
30. M. Littner et al., "Practice parameters for the role of actigraphy in the study of sleep and circadian rhythms: an update for 2002," *Sleep* **26**(3), 337–341 (2003).
31. T. Morgenthaler et al., Committee Standards of Practice, and Medicine American Academy of Sleep, "Practice parameters for the use of actigraphy in the assessment of sleep and sleep disorders: an update for 2007," *Sleep* **30** (4), 519–529 (2007).
32. B. Resnick and E. Galik, "The reliability and validity of the physical activity survey in long-term care," *J. Aging Phys. Act.* **15**(4), 439–458 (2007).
33. G. B. Moody et al., "Clinical validation of the ECG-derived respiration (EDR) technique," *Group* **1**, 3 (1986).
34. G. B. Moody et al., "Derivation of respiratory signals from multi-lead ECGs," *Comput. Cardiol.* **12**, 113–116 (1985).
35. A. Taddei et al., "The European ST-T database: standard for evaluating systems for the analysis of ST-T changes in ambulatory electrocardiography," *Eur. Heart J.* **13**(9), 1164–1172 (1992).
36. N. J. Holter, "New method for heart studies continuous electrocardiography of active subjects," *Science* **134**, 1214–1220 (1961).
37. B. Xhyheri et al., "Heart rate variability today," *Prog. Cardiovasc. Dis.* **55**(3), 321–331 (2012).
38. R. J. Thomas et al., "An electrocardiogram-based technique to assess cardiopulmonary coupling during sleep," *Sleep* **28**(9), 1151–1161 (2005).
39. G. Bonmassar et al., "Motion and ballistocardiogram artifact removal for interleaved recording of EEG and EPs during MRI," *Neuroimage* **16**(4), 1127–1141 (2002).
40. G. E. Strangman, Q. Zhang, and Z. Li, "Scalp and skull influence on near infrared photon propagation in the Colin27 brain template," *NeuroImage* **85**(1), 136–149 (2014).
41. Q. Zhang, G. E. Strangman, and G. Ganis, "Adaptive filtering to reduce global interference in non-invasive NIRS measures of brain activation: How well and when does it work?" *Neuroimage* **45**(3), 788–794 (2009).
42. Q. Zhang, E. N. Brown, and G. E. Strangman, "Adaptive filtering to reduce global interference in evoked brain activity detection: a human subject case study," *J. Biomed. Opt.* **12**(6), 064009 (2007).
43. Q. Zhang, E. N. Brown, and G. E. Strangman, "Adaptive filtering for global interference cancellation and real time recovery of evoked brain activity: a Monte Carlo simulation study," *J. Biomed. Opt.* **12**(4), 044014 (2007).
44. G. E. Strangman, Z. Li, and Q. Zhang, "Depth sensitivity and source-detector separations for near infrared spectroscopy based on the Colin27 brain template," *PLoS One* **8**(8), e66319 (2014).
45. A. F. Arnsten, M. J. Wang, and C. D. Paspalas, "Neuromodulation of thought: flexibilities and vulnerabilities in prefrontal cortical network synapses," *Neuron* **76**(1), 223–239 (2012).
46. A. Harris, T. Hare, and A. Rangel, "Temporally dissociable mechanisms of self-control: early attentional filtering versus late value modulation," *J. Neurosci.: Off. J. Soc. Neurosci.* **33**(48), 18917–18931 (2013).
47. Y. Kubota et al., "Dorsolateral prefrontal cortical oxygenation during REM sleep in humans," *Brain Res.* **1389**, 83–92 (2011).
48. D. T. Delpy et al., "Estimation of optical pathlength through tissue from direct time of flight measurement," *Phys. Med. Biol.* **33**(12), 1433–1442 (1988).
49. M. Hiraoka et al., "A Monte Carlo investigation of optical pathlength in inhomogeneous tissue and its application to near-infrared spectroscopy," *Phys. Med. Biol.* **38**(12), 1859–1876 (1993).
50. J. Choi et al., "Noninvasive determination of the optical properties of adult brain: near-infrared spectroscopy approach," *J. Biomed. Opt.* **9**(1), 221–229 (2004).
51. P. S. Hamilton and W. J. Tompkins, "Quantitative investigation of QRS detection rules using the MIT/BIH arrhythmia database," *IEEE Trans. Biomed. Eng.* **BME-33**(12), 1157–1165 (1986).
52. P. L. Madsen et al., "Cerebral oxygen metabolism and cerebral blood flow in man during light sleep (stage 2)," *Brain Res.* **557**(1–2), 217–220 (1991).
53. P. L. Madsen et al., "Cerebral O2 metabolism and cerebral blood flow in humans during deep and rapid-eye-movement sleep," *J. Appl. Physiol.* **70**(6), 2597–2601 (1991).
54. A. Matsuo et al., "Changes in cerebral hemoglobin indices in obstructive sleep apnea syndrome with nasal continuous positive airway pressure treatment," *Sleep Breathing* **15**(3), 487–492 (2011).
55. T. Nasi et al., "Cyclic alternating pattern is associated with cerebral hemodynamic variation: a near-infrared spectroscopy study of sleep in healthy humans," *PLoS One* **7**(10), e46899 (2012).
56. C. O. Olopade et al., "Noninvasive determination of brain tissue oxygenation during sleep in obstructive sleep apnea: a near-infrared spectroscopic approach," *Sleep* **30**(12), 1747–1755 (2007).
57. M. L. Pierro et al., "Phase-amplitude investigation of spontaneous low-frequency oscillations of cerebral hemodynamics with near-infrared spectroscopy: a sleep study in human subjects," *NeuroImage* **63**(3), 1571–1584 (2012).
58. S. Shiotsuka et al., "Cerebral blood volume in the sleep measured by near-infrared spectroscopy," *Psychiatry Clin. Neurosci.* **52**(2), 172–173 (1998).
59. A. J. Spielman et al., "Intracerebral hemodynamics probed by near infrared spectroscopy in the transition between wakefulness and sleep," *Brain Res.* **866**(1–2), 313–325 (2000).
60. R. E. Brown et al., "Control of sleep and wakefulness," *Physiol. Rev.* **92**(3), 1087–1187 (2012).

Quan Zhang is an instructor in psychology at Harvard Medical School and the director of the Biomedical Engineering Lab at the Neural Systems Group, Massachusetts General Hospital. He has 20 years of experience developing innovative devices for biomedical applications. His recent research includes wearable neuro-monitoring and neuroimaging, and their applications in various clinical and space applications.

Vladimir Ivkovic is a postdoc research fellow at Massachusetts General Hospital and Harvard Medical School. He is a cognitive

neuroscientist and currently focuses on the applications of long-term wearable neuro-monitoring and neuroimaging.

Gang Hu is a biomedical engineer and instructor at Harvard Medical School and Massachusetts General Hospital. He has 10 years of experience developing innovative devices for biomedical applications. In the recent year, he has been focusing on the technology development for wearable neuro-monitoring and neuroimaging.

Gary E. Strangman is an associate professor in the Department of Psychiatry at Harvard Medical School, Director of the Neural Systems Group at Massachusetts General Hospital, and team leader of the NSBRI's Smart Medical Systems and Technology team. His research focuses on translational neuroscience, developing novel neuroimaging technologies for use in operational and clinical environments. He has been PI on multiple NASA, DOD, and NIH grants.